**Proceedings of Proceedings of the ASME 2017 International Design Engineering Technical Conferences &
Computers and Information in Engineering Conference
IDETC/CIE 2017
August 6-9, 2017, Clevland, Ohio, USA**

DETC2017-67942

UNDERSTANDING POWER LOSS DUE TO MECHANICAL ANTAGONISM AND A NEW POWER-OPTIMAL PSEUDOINVERSE FOR REDUNDANT ACTUATORS

Nathan M. Cahill*
Student Researcher
National Science Foundation Fellow
Email: nathan.m.cahill@asu.edu
Thomas Sugar
Professor
Senior Member, ASME
Department of Mechanical Engineering
Arizona State University
Tempe, Arizona 85281

Matthew Holgate
Owner/Researcher
Kyle Schroeder
Researcher
SpringActive inc.
Tempe, Arizona, 85281

ABSTRACT

Comparatively slow growth in power storage and generation makes power-efficient designs desirable for legged robot systems. One important cause of power losses in robotic systems is the mechanical antagonism phenomenon, i.e. one or more motors being used as brakes while the others exert positive energy. This two-part paper first develops a rigorous understanding of mechanical antagonism in multiactuator robotic limbs. We show that, for a 6-DoF robot arm, there exist 4096 distinct regions in the force-velocity space of the end effector (the regions are distinguishable by the sign of the actuator powers). Only sixty-four of these regions correspond with operating points where all actuators exert positive power into the system. In the second part of the paper, we formulate a convex optimization problem which minimizes mechanical antagonism in redundant manipulators. We solve the optimization problem which becomes the derivation for a new, power-optimal, pseudoinverse for non-square Jacobians. In fact, two such pseudoinverses are derived: one for statically determinate systems, such as serial manipulators, and one for statically indeterminate systems, such as parallel manipulators.

*Address all correspondence to this author.

1 INTRODUCTION

State-of-the-art legged robot systems are less energy efficient and less powerful than their biological counterparts. Their progress has been bottlenecked by relatively slow growth in power storage and generation technologies. To counteract this slow growth, research must be focused on reducing power losses in legged systems. This explores a phenomenon, called mechanical antagonism, whereby multiactuator robot arms waste considerable power due to an effect first mentioned by Waldron and Kinzel's early work [1]. In [2], Abate et al. resurrected this work showing that even cutting edge robotic systems suffer significant losses due to this phenomenon. The contributions of this paper are twofold. We first reveal the directional nature of antagonistic power losses in robotic arms, using a 2-DoF robot manipulator for demonstration. Specifically, we partition the end effector space into geometric regions using concepts from screw theory, and identify the antagonistic regions. We then present suggestions on how to avoid mechanical antagonism in designs for performance-driven multiactuator robotic limbs. In the second part of the paper, we present a new pseudoinverse for over-actuated robot arms that minimizes losses due to mechanical antagonism.

We argue that energy efficiency and power density should

be chief concerns for robot developers. As evidence of this, we turn to the growth rate of various technologies. The performance of power storage and generating machines has not been growing at the same rate as information technology. This is well known, and has also been documented in literature [3]–[6].

The motivation to progress the state of the art in legged vehicles comes mainly from their impressive potential in biology. Assistive robots must be capable of navigating the same environments that people do - environments which are built to be traversed by legs. Wheeled systems have difficulty overcoming obstacles which do not present a problem for legs. Uneven terrain is among the foremost. These obstacles exist even indoors, in the form of steps or debris. Many impressive robotic systems have been developed with capabilities to traverse uneven terrain, but none is as powerful and/or efficient as its biological counterpart. Robotic systems such as BigDog [7], and Honda's Asimo [8] are capable of dynamic balancing and traversing rugged terrain, but these capabilities come at the cost of energy efficiency. Other robots such as Cornell University's Ranger [9] have extreme energy economy but are not designed for rugged terrain navigation.

Many groups are attempting to build robotic systems that have both high performance and energy efficiency. For example, Hurst et al. [10]–[12] has developed an efficient bipedal robot, Atrias, that is capable of navigating rough terrain. The design focuses on utilizing the natural dynamics of the robot in a way that will help them save energy step to step [13], [14]. Nonetheless, a weakness of the leg structure was recently discovered: the robot loses considerable power due to mechanical antagonism due to its pantograph leg mechanism [2].

The MIT cheetah robot created by Kim et al. has also made significant progress towards efficient and robust legged navigation [15], [16]. The mechanical design of the legs is a planar serial robot. The group designed the robot with a planar leg mechanism which is stiff and light. Their low impedance design is meant to regenerate energy from braking through the motors, but efficiently regenerating power back into the batteries of a DC motor actuation system is difficult, at best. Kim et al., with custom designed motors, achieve the braking process with an efficiency of only 63 percent [15]. While some amount of braking energy during gait may be unavoidable, the authors approach is to circumvent the problem by specialization of the design of the limb.

The authors show the viability of this approach in a pair of published works [17], [18]. In the first paper, a hybrid serial-parallel actuation approach is introduced. In the second paper, Cahill et al. show that the geometry of spatial mechanism may be tuned to a given data set, sufficiently eliminating losses to antagonistic power [18]. Designing the kinematics to avoid actuator antagonism in this way avoids the inefficiencies inherent to energy regeneration, whether by DC generators or springs. Avoiding antagonism not only reduces the need for regeneration; in many cases it also reduces the peak motor powers associated with a task. This is because, like any thermodynamic system, power-in equals power-out. Assuming for the moment that the limb is being used to produce positive work at the end-effector, when the mechanical antagonism phenomenon occurs, one or more actuators has become a power *sink*, instead of a power *source*. This means that the remaining power source actuators must provide the sum of the output energy demanded by the end effector *and* the energy being sunk into the antagonistic actuators. Depending on the task, this may dramatically increase the value of peak instantaneous power and current required. This, in turn, will lead to larger motors and more expensive power inverters.

This paper is structured as a three part paper. The first part, described in Section 2, uses a visual method to introduce the phenomenon and to show how the kinematics of the limb, as well as the directionality of the task, can cause mechanical antagonism. Next, in Section 3, we derive a power-optimal pseudoinverse for over-actuated systems which minimizes antagonistic motor power for both statically determinate and statically indeterminate systems. Finally, in Section 4, we validate the power-optimal pseudoinverse using a model of a three DoF over-actuated planar serial manipulator.

2 Mechanical Antagonism Visualized at the End Effector

This section gives a series of steps which help to understand the mechanical antagonism phenomenon in an intuitive and visual way. We introduce a planar two DoF serial robotic limb. This planar limb can move its end effector linearly in any direction on the plane. Also, it is capable of applying a force in any direction on the plane but we restrict the robot from applying a moment normal to the plane (imagine a bearing at the end effector). This robot limb is shown in Figure 1. In order to visualize mechanical antagonism in this system, the velocity space and the force space of the end effector, as well as the screws/wrenches which form the basis for these vector subspaces, will be shown in detail. Finally, these two spaces combine to form the force-velocity vector space in $\mathbb{R}^4$. This vector subspace is split into contiguous motor power regions distinguished by the sign of the power generated at each motor. Only a small subset of these regions are non-antagonistic. The goal is to reduce the multiactuator robot limb's power consumption by avoiding

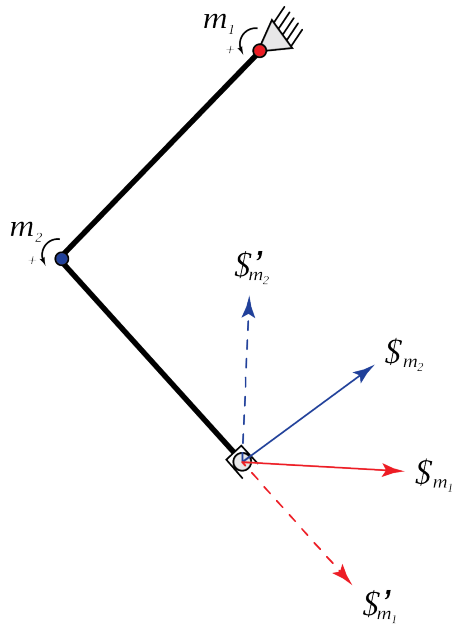

FIGURE 1. Diagram of the serial limb robot. Also shown are the basis vectors of the velocity and force space.

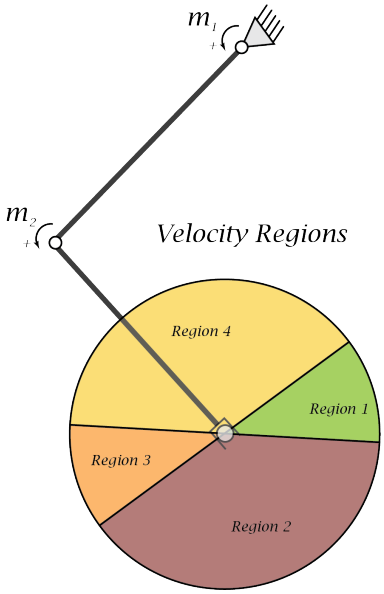

FIGURE 2. Visualizing the velocity space of the robot leg

the regions with poor efficiency, or by designing the robot to fit the desired task.

2.1 Visualizing the Velocity Space

The velocity space of a robot limb is the column space of the leg Jacobian. It is a vector space that contains all of the velocity vectors that the end effector is theoretically capable of achieving (it does not account for any actuator limitations), and each of the columns corresponds to a specific actuator (column one with motor one, column two with actuator two, etc.). The example robot chosen allows us to visualize the velocity space, and particularly the borders between the regions.

The first column of the Jacobian is the two-dimensional screw associated with motor one (notated as $\$_{m_1}$). It represents the end effector velocity corresponding to a unit input from motor one and zero input from motor two (e.g., motor two fixed). This vector is perpendicular to a line drawn between joint one and the end effector (see Figure 1). Similarly the second column in the Jacobian (notated as $\$_{m_2}$) describes the velocity of the end effector when motor two is excited with a unit velocity and motor one is held fixed. This vector is perpendicular to a line between the end effector and joint two. These two vectors are basis vectors for the motor velocity space, meaning a velocity of any magnitude in any direction in the plane can be formed via a linear combination of the two:

$$\$_{EE} = \dot{q}_{m_1}\,\$_{m_1} + \dot{q}_{m_2}\,\$_{m_2}. \tag{1}$$

Where $\dot{q}_{m_1}$ and $\dot{q}_{m_2}$ are the velocity magnitudes of motors one and two respectively. Also, $\$_{EE}$ is the velocity of the end effector. Equation 1 is just a rewritten form of the well-known Jacobian equation:

$$\$_{EE} = J\,\dot{q}. \tag{2}$$

Where $\dot{q}$ is a 2x1 vector of the motor velocities, and J is the Jacobian.

A "region" of the velocity space is a contiguous set of vectors in which the signs of the motor velocities in Equation 1 do not change. Figure 2 shows the four important regions of the velocity space for this leg, and Table 1 details what each region represents. For example, region one is the set of end effector directions that correspond to motor one and motor two moving in a positive direction (see row one of Table 1). The edges of each region correspond to zero crossings of one motor or the other. For example, the edge between region one and region two is along the vector $\$_{m_1}$. This vector represents a zero crossing for motor two. These velocity regions are an important component in determining which directions a given robot's antagonistic power regions will lie. To determine the sign of the motor coordinates in each region, one must look at the direction of the vectors $\$_{m_1}$ and $\$_{m_2}$. For example, a velocity parallel with the vector $\$_{m_1}$ will by definition require a positive velocity at motor one (and a zero velocity from motor two). The sign of motor one's velocity is positive in any direction that is not separated from $\$_{m_1}$ by a motor one zero crossing (zero crossings for motor one happen at $\pm\$_{m_2}$). This means motor

one has a positive velocity value in regions one and two, and a negative value in regions three and four. Following this same line of thought, motor two will have a positive velocity in regions one and four and a negative value in regions two and three.

TABLE 1. Velocity Regions

	Sign: $\dot{q}_{m_1}$	Sign: $\dot{q}_{m_2}$
Region One	+	+
Region Two	+	-
Region Three	-	-
Region Four	-	+

It may be noted that the four regions defined in this discussion are a mapping of the four quadrants of a two-dimensional Cartesian coordinate system having motor one velocity on one axis and motor two velocity on the other. The Jacobian matrix maps these four coordinates onto the end effector space. This discussion is meant to give an intuitive and visual understanding of how that mapping works, because this mapping has a large impact on the efficiency of the system for a given task. In the next section, the visualization of the force space will be detailed.

2.2 Visualizing the Force Space

The force space of the leg can be visualized much in the same way as the velocity space. It is the column space of the inverse transpose of the leg Jacobian (assuming the Jacobian is invertible and there are no energy losses to friction). To begin visualizing this space, imagine a unit torque is applied through motor one but motor two is free. Since no moment can be transferred through joint two or the end effector, the force contribution of motor one ($\$'_{m_1}$) can be drawn starting at the end effector and pointing away from joint two (represented by the red dotted line in Figure 1). The direction of this vector is determined by the assigned direction of positive torque about motor one. The force contribution of motor two can be drawn in the same way. Its line of action must lie on a line that contains the end effector and joint one (it is shown as a blue dotted line in Figure 1. These are the basis vectors of the force space. Similar to Equation 1, the end effector output force ($\$'_{EE}$) can be written as:

$$\$'_{EE} = \tau_{m_1}\,\$'_{m_1} + \tau_{m_2}\,\$'_{m_2}. \tag{3}$$

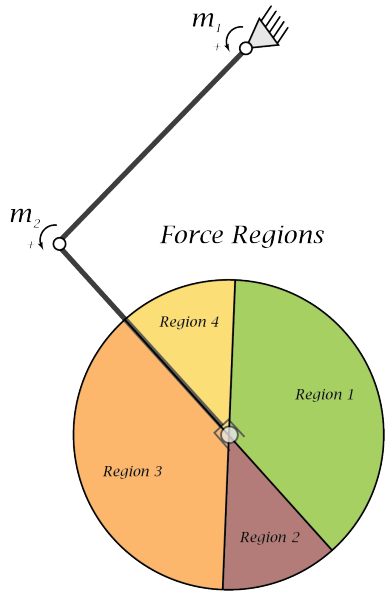

FIGURE 3. Visualizing the Force Space of the robot leg

In this case, $\$'_{EE}$ is a 2x1 vector containing the components of the end effector force. As in the above discussion Equation 3 is a rewritten form of the well-known equation:

$$\$'_{EE} = (J^T)^{-1}\,\tau. \tag{4}$$

It should be noted here that the Jacobian must be invertible to write this equation. In this case, the matrix is square, and as long as the robot is not in a singular position, the Jacobian will be invertible. In Section 3 we discuss over-actuated systems and their implications on antagonistic power. Figure 3 shows the four regions of the velocity space

TABLE 2. Force Regions

	Sign: τ_{m_1}	Sign: τ_{m_2}
Region One	+	+
Region Two	+	-
Region Three	-	-
Region Four	-	+

for this leg, and Table 2 details what each region represents. A region in the force space, similar to those of the velocity space, corresponds to a contiguous set of end effector forces which have a particular combination of motor torque signs. For example, region one encompasses all the end effector

force directions which correspond to both motors having positive torque values. The signs of the motor force change at zero crossings. This means that the edges of each region represent end effector force directions in which one motor contributes zero force. These zero crossing directions correspond to the vectors $\$'_{m_1}$ and $\$'_{m_2}$, shown in Figure 1 - $\$'_{m_1}$ being a zero crossing for motor two and $\$'_{m_2}$ being a zero crossing for motor one. In this way the columns of the inverse transpose leg Jacobian create the edges of the four regions of the leg force space. These regions are constructed using the same process as explained in Section 2.1. Determining the sign of the motor forces in these regions can be accomplished in a similar method as described in Section 2.1. By definition the sign of the torque value at motor one is positive when end effector force is pointing in the direction of $\$'_{m_1}$. This sign will not change as the angle between the end effector force and $\$'_{m_1}$ increases unless a zero crossing for motor one occurs. These zero crossings happen when the end effector force is aligned with $\pm\$'_{m_2}$. Using this method, it becomes apparent that regions one and two correspond to positive torque values for motor one. Therefore, regions three and four have negative torque values for motor one. In a similar manner, motor two has positive values in regions one and four and a negative value in regions two and three.

2.3 The Force-Velocity Space

Since actuators can apply forces and velocities independently, the force space and the velocity space can be combined into a four-dimensional force-velocity space. This force-velocity space is the space that is of interest. One point in this space specifies the velocity direction and magnitude, as well as the force direction and magnitude. It is useful to define this space for the discussion. There are two coordinate frames of interest. The global coordinate frame χ has the end effector forces and velocities:

$$\chi = \begin{bmatrix} \$_{EE} \\ \$'_{EE} \end{bmatrix}. \tag{5}$$

The other frame of interest is the local or motor coordinate frame ξ, which has $\dot{q}$ and τ:

$$\xi = \begin{bmatrix} \dot{q} \\ \\ \tau \end{bmatrix} = \begin{bmatrix} \dot{q}_{m_1} \\ \dot{q}_{m_2} \\ \tau_{m_1} \\ \tau_{m_2} \end{bmatrix} \tag{6}$$

The Jacobian can be used as a coordinate transformation between the two coordinate systems:

$$\chi = \begin{bmatrix} J\,\dot{q} \\ (J^T)^{-1}\,\tau \end{bmatrix} \tag{7}$$

One transformation matrix ($\mathcal{J}$) can be built from the Jacobians which maps the forces and velocities from actuator frame to the end effector frame.

$$\mathcal{J} = \begin{bmatrix} J & \underline{0} \\ \underline{0} & (J^T)^{-1} \end{bmatrix}. \tag{8}$$

Which allows:

$$\chi = \mathcal{J}\,\xi. \tag{9}$$

The four coordinates of the force-velocity space of the leg contain all the necessary information to know which regions are antagonistic and which regions are not. To define the antagonistic power regions, power must be formulated.

2.4 Power

Mechanical power (P) is a function of only velocity and force. Due to this, every point in the force-velocity space is associated with a specific overall power output. This power output can be formulated as:

$$P = \$_{EE}^T\,\$'_{EE} \tag{10}$$

Where P is the mechanical power output at the end effector. Since we are assuming no losses, power-in equals power-out, and the sum of the individual motor powers (P_{m_1} and P_{m_2}) is equal to P as well.

$$P = \tau^T\dot{q} = P_{m_1} + P_{m_2} \tag{11}$$

Note that the sign of the motor powers will be determined by the product of the motor torques and velocity. We have just shown that these are a function of the direction of desired end effector torque and velocity. Imagine, for example, that the desired power at the end effector is positive and in a direction that causes the power at motor one to be negative. If this is the case, motor two will have to produce power equivalent to the sum of the magnitude of the power at motor one *and* the end effector power requirement. This is the phenomenon of interest - mechanical antagonism - and it is undesirable for more than one reason: firstly, because it will raise the peak power requirement of the task, resulting in the need for larger motors in the design; secondly, because inevitably, energy will be lost to heat by the motor which is performing braking (not to mention the heat losses due to the added work on the positive power motor). One could argue that the energy could be regenerated through the motor and stored back into the battery for later use, but the regeneration process is currently very inefficient, and much of the energy will be wasted. Regardless of this, reducing the antagonistic power will increase the power density of the system, which is a very valuable result considering the slow growth of power technology. The next section will detail

which regions in the torque velocity space are associated with mechanical antagonism.

2.5 Antagonistic Power Regions

Antagonistic power regions are those which the sign of the product of torque and velocity for one motor does not match the other(s). Since, as noted above, the torque and velocity of an actuator are generally independent, every combination of the regions from Table 1 and 2 is possible. This means there are 16 distinct regions in the force-velocity space. Since even for this simple example the space is four-dimensional, a figure displaying the regions directly is too complicated. Instead the 16 regions are displayed in Table 3. Each row corresponds to a region of Figure 2, and defines which of the regions in Figure 3 are antagonistic. For example, if one desired to move the end effector vertically downward, to avoid mechanical antagonism, a force may only be applied in the direction of Region 2 of Figure 3.

TABLE 3. Power regions

Velocity	Force			
	Region 1	Region 2	Region 3	Region 4
Region 1				
P_{m_1}	+	+	-	-
P_{m_2}	+	-	-	+
Region 2				
P_{m_1}	+	+	-	-
P_{m_2}	-	+	+	-
Region 3				
P_{m_1}	-	-	+	+
P_{m_2}	-	+	+	-
Region 4				
P_{m_1}	-	-	+	+
P_{m_2}	+	-	-	+

It should be noted that only four of these regions are "positive power regions", or regions which correspond to positive power output for both actuators. Of the twelve other regions eight correspond with antagonistic power regions, and four correspond with both motors braking. If the end effector is used to dampen energy out of the system then the braking regions would be the desirable ones. Otherwise the goal would be to keep the robot operating in the "positive power regions". This may be accomplished by changing the task to fit the robot or, by designing the kinematics of the robot especially for the intended task. The latter is the approach taken by the author and published in in a 2016 paper [17].

This completes the detailed force-velocity analysis of this robot arm. Every robot limb has a force-velocity space. Some of these spaces are more complex than others. For every degree of freedom added to the robot two degrees of freedom are added to the force-velocity space. For example, imagine a third actuator was added to the end effector of the above example. This would allow the arm to control not only linear velocities and forces but also the rotational velocity and torque output. The force-space would be six dimensional, with eight (2^3) force and eight velocity regions, making 64 distinct power regions, of which eight are non-antagonistic positive power regions. A robot arm that operates in six-dimensional space (three linear dimensions and three rotational dimensions) has a 12-dimensional force-velocity space with 64 (2^6) force and 64 velocity regions. This means there are 4096 distinct regions but *only 64 of these are non-antagonistic positive power regions.*

3 Power-Optimal Pseudoinverses for Redundant Manipulators

It is of interest to extend this analysis to over-actuated robotic systems. These systems have non-square Jacobian matrices. Two cases will be presented here. Case one is a system which is statically determinate and has one and only one solution for actuator torque given the desired end-effector torque. This case has infinite solutions for actuator velocities given desired end-effector velocities. This case is applicable to redundantly actuated serial manipulators. Case two is a system which is statically indeterminate, meaning there are infinite combinations of actuator forces which produce the desired motor torque but there is only one solution for actuator velocity. This case is applicable to redundantly actuated parallel robots. Both of these cases will be discussed here along with a power-optimal pseudoinverse.

3.1 Case 1: Statically Determinate Manipulators

In the case of statically determinate manipulators, such as redundant serial limbs, the J will have dimension $n \times m$, where $m > n$. Equations 2 still holds, but now J is not invertible so Equation 4 does not. There are infinite solutions to Equation 2 for $\dot{q}$ given $\$_{EE}$. The classical solution to this problem is the so-called pseudoiverse of the Jacobian:

$$J^{\dagger} = J^T \left(J \, J^T \right)^{-1}. \tag{12}$$

This solution minimizes the sum of squares of the motor velocities. In light of mechanical antagonism, this solution

does not seem ideal. Small motor velocities are not as important as the reduction of antagonistic motor power. The ideal solution therefore will minimize the sum of square motor powers. Fortunately, an analytical solution exists which accomplishes this goal. We formulate the problem as follows:

$$\begin{aligned} \min: &\quad P^T P \\ \text{s.t.}: &\quad \$_{EE} = J\dot{q} \end{aligned}$$

Where P is a vector of motor powers,

$$P = diag(\tau)\dot{q}. \tag{13}$$

The power vector is a product of a matrix, $diag(\tau)$ the diagonal of the motor torques and the motor velocity vector. We will give the diagonal torque matrix a more convenient convention, T, for the remainder of the analysis. The equation for sum of square power can be written as:

$$P^T P = \dot{q}^T \mathrm{T}^2 \dot{q} \tag{14}$$

Next we solve the optimization problem, starting by constructing the Lagrangian:

$$L = \frac{1}{2}\dot{q}^T \mathrm{T}^2 \dot{q} + \lambda^T (J\dot{q} - \$_{EE}) \tag{15}$$

The minimum of Equation 15 can be found by equating the gradient of the function to zero. The gradient of this function is as follows:

$$\nabla L = \begin{bmatrix} \frac{\delta L}{\delta \dot{q}} \\ \\ \frac{\delta L}{\delta \lambda} \end{bmatrix} = \bar{0} \tag{16}$$

Where:

$$\frac{\delta L}{\delta \dot{q}} = \mathrm{T}^2 \dot{q} + J^T \lambda, \tag{17}$$

and

$$\frac{\delta L}{\delta \lambda} = J\dot{q} - V. \tag{18}$$

Equation 17 may be solved for $\dot{q}$:

$$\dot{q} = -\mathrm{T}^{-2} J^T \lambda. \tag{19}$$

Since the square of a diagonal matrix is a positive definite matrix T^2, which will always be invertible. Equation 19 may now be substituted into Equation 18 and solved for λ giving:

$$\lambda = -(J\,\mathrm{T}^{-2} J^T)^{-1} \$_{EE}. \tag{20}$$

If J has full row rank, the quantity $(J\,\mathrm{T}^{-2} J^T)$ will be invertible. The power-optimal motor joint velocity $(\hat{\dot{q}})$ results from substituting Equation 20 into 19:

$$\hat{\dot{q}} = \mathrm{T}^{-2} J^T (J\,\mathrm{T}^{-2} J^T)^{-1} \$_{EE} \tag{21}$$

The power-optimal pseudoinverse $(\hat{J})$ results from Equation 21:

$$\hat{J} = \mathrm{T}^{-2} J^T (J\,\mathrm{T}^{-2} J^T)^{-1}. \tag{22}$$

Using this pseudoinverse of the nonsquare Jacobian matrix will guarantee that antagonistic power is minimized, given a desired end effector velocity and an expected motor torque matrix. Note that T^2 is the square of a diagonal matrix. This means the objective here is positive semi-definite and, since the constraints are linear, the problem is convex.

3.2 Case 2: Statically Indeterminate Manipulators

Case two differs from case one in that for statically indeterminate manipulators, such as redundant parallel robots, there are infinite combinations of actuator torques (τ) which produce the desired end effector torque $(\$'_{EE})$. The formulation of the optimization problem becomes:

$$\begin{aligned} \min: &\quad P^T P \\ \text{s.t.}: &\quad \$'_{EE} = J'\tau \end{aligned}$$

The solution to the problem follows the same form as the previous solution:

$$\hat{J}' = \mathrm{W}^{-2} J'^T (J'\,\mathrm{W}^{-2} J'^T)^{-1}. \tag{23}$$

Where W is a diagonal weighting matrix containing the joint velocities. This solution is guaranteed to be the global solution to the problem because the problem is convex. This is due, as previously stated, to the fact that the weighting matrix - in this case W^2 - is a positive semi-definite matrix and the constraints are linear.

4 Validation Using Redundant Serial Limb

In effort to verify the optimal solutions presented above, we will consider a three DoF planar serial robot arm.Similar to Section 2, the robot may move in two-dimensions and apply force in two-dimensions. Torque at the end effector is constrained to zero. This means the system has one redundant DoF.

The Jacobian of this manipulator has dimension two by three. Three actuators produce velocities in a three dimensional space which projects onto the two-dimensional end effector velocity space. Given a desired end effector velocity, infinite solutions exist in the three dimensional actuator velocity space which can create the desired velocity. Section 3.1 derives the solution within the infinite possibilities which minimizes the sum of square power (or SSP).

As a case study, we chose arbitrary desired end effector force and velocity directions. Then we reduced the system of

linear equations (from Equation 2) to two equations which define the velocity of actuators one and two as a function of actuator three velocity. Finally, we made a plot of the SSP vs a range of actuator three velocities which satisfy the conditions. Figure 4 shows this plot, including the location of the classical minimal velocity pseudoinverse and the power optimal pseudoinverse solutions. It should be noted that the power optimal solution lies at the minimum of the function while the classical solution lies at a point with smaller velocity, but larger SSP.

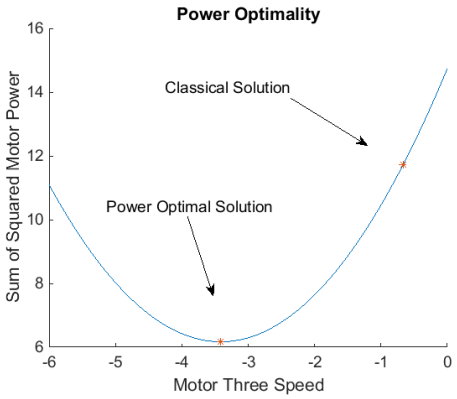

FIGURE 4. Plotting the cost function over the constrained problem space.

5 Conclusions

In this two-part paper, we first rigorously developed the force-velocity space of a multiactuator robotic arm. We detail the process for a two DoF serial arm to help the reader build intuition for how antagonism develops in multiactuator systems. We emphasized the importance of the directions of the desired end effector force and velocity, and we showed how the kinematics define which directions are efficient and which are not. Antagonistic actuator work is a phenomenon which must not be ignored in the design process of a robotic limb. Designers should know that the directional aspect of a task will determine which force-velocity region it will fall into, and therefore how much energy is lost to mechanical antagonism in the joints. The kinematics of the robot arm have a direct effect on which directions are efficient and which are not. We suggest designing the kinematics of the arm to avoid motor antagonism. An optimization routine like the one in [18] may be implemented to do so.

In the second part of the paper we looked at over-actuated systems, which have non-invertible Jacobians. We show how the added degrees of freedom may be utilized to reduce the effect of mechanical antagonism. This led to analytical solutions which minimize the sum of squares of the mechanical work exerted by the joints in both parallel and serial, redundant mulitactuator robotic arms. We argue that this pseudoinverse is superior to the classical velocity-optimal one. Minimizing actuator work will extend battery life of mobile robots and, if the actuator is a DC motor, reduce the risk of motor failure due to waste heat generated in the windings.

6 Future Work

While this paper has focused on the phenomenon of mechanical antagonism and how to minimize it for redundant systems, there may be a more meaningful solution to the problem. Using an actuator model specific to the robot in question would allow the minimization of electrical power. This model could take into account losses due to inertia, actuator inefficiency, regenerative capabilities, and so on. For this paper, a general solution has been presented which minimizes mechanical antagonism. More specific solutions could be attained minimizing, for example, electrical power consumption, wasted heat in motor windings, or the fuel consumption of the hydraulic pump. If future end effector trajectory is known, the future energy consumption may be considered. In this way, the optimal joint trajectory in the position and velocity space could be determined. Since an abundance of solutions may exist which could be considered the best for one reason or another, we chose to present a simple general solution here. We leave it to future work to further explore this problem and compare this general solution to more specific ones.

While this line of research would be interesting, redundant manipulators may not be the ideal solution to reducing mechanical antagonism. Redundant manipulators are not often used in applications requiring high power to weight ratios. Legged robots, for example, have limbs that are typically under-actuated. This may be due to the fact that redundant actuators add weight and cost to the system. For systems that require high power density, we suggest using optimal design methods to reduce mechanical antagonism and other actuator specific inefficiencies (see [18]).

References

[1] K. J. Waldron and G. L. Kinzel, "The relationship between actuator geometry and mechanical efficiency in robots," *Fourth, __'mposium on Theory and Practice of Robots and Manipulators. Poland*, 1981.

[2] A. Abate, J. W. Hurst, and R. L. Hatton, "Mechanical antagonism in legged robots," presented at the Robotics: Science and Systems XII, 2016.

[3] H. Koh and C. L. Magee, "A functional approach for studying technological progress: Application to information technology," *Technological Forecasting and Social Change*, vol. 73, no. 9, pp. 1061–1083, 2006.

[4] J. D. Farmer and F. Lafond, "How predictable is technological progress?" *Research Policy*, vol. 45, no. 3, pp. 647–665, Apr. 2016.

[5] C. L. Benson and C. L. Magee, "Quantitative determination of technological improvement from patent data," *PLOS ONE*, vol. 10, no. 4, e0121635, Apr. 15, 2015.

[6] C. Benson and C. L. Magee, "On improvement rates for renewable energy technologies: Solar PV, wind turbines, capacitors, and batteries," *Renewable Energy*, vol. 68, 2014.

[7] M. Raibert, K. Blankespoor, G. Nelson, R. Playter, *et al.*, "Bigdog, the rough-terrain quadruped robot," in *Proceedings of the 17th World Congress*, 2008, pp. 10 823–10 825.

[8] M. Hirose and K. Ogawa, "Honda humanoid robots development," *Philosophical Transactions of the Royal Society of London A: Mathematical, Physical and Engineering Sciences*, vol. 365, no. 1850, pp. 11–19, Jan. 15, 2007.

[9] J. Bhounsule, J. Cortell, and A. Ruina, "Design and control of ranger: An energy-efficient, dynamic walking robot," in *Proc. CLAWAR*, 2012, pp. 441–448.

[10] D. Koepl and J. Hurst, "Force control for planar spring-mass running," in *2011 IEEE/RSJ International Conference on Intelligent Robots and Systems (IROS)*, Sep. 2011, pp. 3758–3763.

[11] ——, "Impulse control for planar spring-mass running," *Journal of Intelligent & Robotic Systems*, vol. 74, no. 3, pp. 589–603, Jun. 1, 2014.

[12] H. R. Vejdani, A. Wu, H. Geyer, and J. W. Hurst, "Touch-down angle control for spring-mass walking," in *2015 IEEE International Conference on Robotics and Automation (ICRA)*, May 2015, pp. 5101–5106.

[13] A. Abate, R. L. Hatton, and J. Hurst, "Passive-dynamic leg design for agile robots," in *2015 IEEE International Conference on Robotics and Automation (ICRA)*, IEEE, 2015, pp. 4519–4524.

[14] J. A. Grimes and J. W. Hurst, "The design of ATRIAS 1.0 a unique monoped, hopping robot," in *Proceedings of the 2012 International Conference on Climbing and Walking Robots and the Support Technologies for Mobile Machines*, 2012, pp. 548–554.

[15] S. Seok, A. Wang, M. Y. Chuah, D. Otten, J. Lang, and S. Kim, "Design principles for highly efficient quadrupeds and implementation on the MIT cheetah robot," in *2013 IEEE International Conference on Robotics and Automation (ICRA)*, May 2013, pp. 3307–3312.

[16] S. Seok, A. Wang, D. Otten, and S. Kim, "Actuator design for high force proprioceptive control in fast legged locomotion," in *Intelligent Robots and Systems (IROS), 2012 IEEE/RSJ International Conference on*, IEEE, 2012, pp. 1970–1975.

[17] N. Cahill, "Advanced parallel actuation of a serial robotic leg," presented at the ASME IDETC 2016, Charolette, NC, 2016.

[18] N. Cahill, Y. Ren, and T. Sugar, "Mechanical specialization of robotic limbs," presented at the International Conference on Robotics and Automation, Singapore, May 29, 2017.